Inorganic Chemistry

Article

pubs.acs.org/IC

$Cs(TaO_2)_3(SeO_3)_2$ and $Cs(TiOF)_3(SeO_3)_2$: Structural and Second Harmonic Generation Changes Induced by the Different d^0-TM Coordination Octahedra

Xue-Li Cao,[†,‡] Chun-Li Hu,[†] Fang Kong,[†] and Jiang-Gao Mao*[,†]

[†]State Key Laboratory of Structural Chemistry, Fujian Institute of Research on the Structure of Matter, Chinese Academy of Sciences, Fuzhou 350002, P. R. China

[‡]University of the Chinese Academy of Sciences, Beijing 100039, P. R. China

Supporting Information

ABSTRACT: Two new cesium selenites containing TaO_6 or TiO_4F_2 octahedra, namely, $Cs(TaO_2)_3(SeO_3)_2$ (**1**) and $Cs(TiOF)_3(SeO_3)_2$ (**2**), have been prepared using standard high temperature solid-state method and hydrothermal reaction, respectively. Compound **1** crystallizes in $P\bar{3}m1$ and features an unusual $[(TaO_2)_3(SeO_3)_2]^-$ sandwich-like double layer in which two $[Ta(1)O_3(SeO_3)]^{3-}$ layers are bridged by central $Ta(2)O_6$ octahedra via corner-sharing, whereas $Cs(TiOF)_3(SeO_3)_2$ with a polar space group $P6_3mc$ features an interesting hexagonal tungsten oxide (HTO) layered topology and presents a strong second harmonic generation (SHG) of about 5 × KDP (KH_2PO_4), which is much larger than those of $A(VO_2)_3(QO_3)_2$ (A = K, Tl, Rb, Cs, or NH_4; Q = Se, Te) with a similar HTO layered structure. $Cs(TiOF)_3(SeO_3)_2$ is also type-I phase matching. The SHG of above-mentioned HTO materials can be enhanced greatly with the replacement of VO_6 octahedra by TiO_4F_2 octahedra. Furthermore, thermal stabilities, UV−vis diffuse reflectance spectra, infrared spectra, relationship between crystal structure and SHG, and theoretical calculations were also reported.

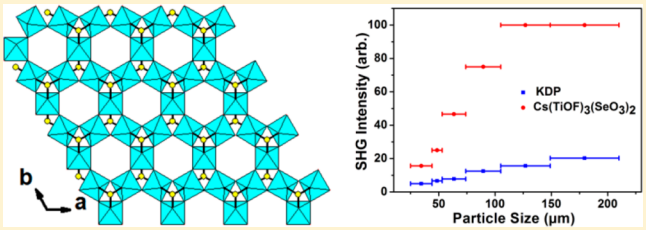

INTRODUCTION

Selenites and tellurites have been widely developed over the last two decades for their rich structural chemistry and useful physical properties. Se^{4+} and Te^{4+} cations with a stereoactive lone-pair are impressionable to second-order Jahn−Teller (SOJT) distortion, which is in favor of forming a noncentrosymmetric (NCS) framework with conceivable second harmonic generation (SHG).[1] Research also indicates that it is an effective synthetic route to design new NCS structures by introducing the octahedrally coordinated transition metal (TM) into metal selenite and tellurite systems.[2,3] The d^0 electronic configuration TMs, such as V^{5+} (Ti^{4+}, W^{6+}, Mo^{6+}, Nb^{5+}, Ta^{5+}), are also sensitive to SOJT distortion, which can improve the possibility of obtaining the NCS structures. Furthermore, several d^0-TM cations can adopt various coordination geometries such as MO_4, MO_5, and MO_6 (M = Mo, V, etc.), which can be further interconnected into all kinds of skeletons, such as isolated polynuclear clusters, 1D chains, and 2D layers, as well as 3D frameworks, affording a rich structural chemistry.[2,3]

Selenite- or tellurite-based hexagonal tungsten oxide (HTO) materials are the typical layered selenites or tellurites containing d^0-TM.[4−7] Many of these HTOs are macroscopically polar due to local polarity "constructively adding" from octahedrally coordinated d^0-TM, such as Mo^{6+}, W^{6+}, V^{5+}, Ti^{4+}, Ta^{5+}, as well as Nb^{5+}, and the cations with a lone-pair, such as Se^{4+} and Te^{4+}, and they can exhibit various important functional properties, such as SHG, piezoelectricity, ferroelectricity, as well as pyroelectricity.[8,9] For the polar HTOs, the distorted octahedra of d^0-TM form anionic layers, which are capped by selenite $(SeO_3)^{2-}$ or tellurite $(TeO_3)^{2-}$ groups from one or both sides.[4a] The polar HTO-type oxides are divided into two forms: class 1 ("capped" on both sides) and class 2 ("capped" on one side). Class 1 HTO-type materials include $A(V^{5+}O_2)_3(SeO_3)_2$ (A = NH_4^+, K^+, Rb^+, Cs^+, or Tl^+)[4b,6a−c] and $Cs(V^{5+}O_2)_3(TeO_3)_2$,[6d] and they display only weak SHG responses of about 30−50 × α-SiO_2; class 2 HTO-type materials include $A_2(Mo^{6+}O_3)_3(SeO_3)$ (A = NH_4^+, Rb^+, Tl^+, or Cs^+),[3a,7a] $A_2(Mo^{6+}O_3)_3(TeO_3)$ (A = NH_4^+ or Cs^+),[7b] $A_2(W^{6+}O_3)_3(SeO_3)$ (A = NH_4^+ or Cs^+),[7c] and $Rb_2(W^{6+}O_3)_3(TeO_3)$,[4c] and they can exhibit large SHG responses of about 300−400 × α-SiO_2, which can be explained by the alignments of the polarizations from their selenite or tellurite groups.

Recently, we have focused on the Pb^{2+}−(d^0-TM)−Se^{4+}−oxyhalide system due to the fact that halide atoms prefer to coordinate with TM rather than Se^{4+} cation, leading to the formation of many low dimensional materials.[10] Four compounds have been obtained, namely, $Pb_2TiOF(SeO_3)_2Cl$, $Pb_2NbO_2(SeO_3)_2Cl$, $Pb_2VO_2(SeO_3)_2Cl$, and $PbVO_2(SeO_3)F$,

Received: January 7, 2015
Published: April 2, 2015

DOI: 10.1021/acs.inorgchem.5b00052
Inorg. Chem. 2015, 54, 3875−3882

among which $Pb_2TiOF(SeO_3)_2Cl$ shows a strong SHG of 9.6 × KDP.[11a] Results from our DFT theoretical calculations also demonstrate that the introduction of F^- into the d^0-TM coordination sphere can change the band structures and then lead to the large SHG enhancement. On account of this interesting indication, our current research focuses on the introduction of F^- anion into the d^0-TM coordination sphere of the HTO materials based on d^0-TM selenites. In this field, we successfully obtained two new mixed metal selenites, namely, $Cs(TaO_2)_3(SeO_3)_2$ (**1**) and $Cs(TiOF)_3(SeO_3)_2$ (**2**). Compound **2** shows a HTO-type layered structure similar to that of $A(V^{5+}O_2)_3(QO_3)_2$ (A = NH_4^+, K^+, Rb^+, Cs^+, or Tl^+; Q = Se, Te);[4b,6a−c] however, it presents a much larger SHG of approximately 5 × KDP compared with those of 30−50 × α-SiO_2 for $A(V^{5+}O_2)_3(QO_3)_2$. Hereupon, we will perform the syntheses, structures, optical properties, studies of the relationship between crystal structure and SHG, as well as DFT calculations.

EXPERIMENTAL SECTION

Materials and Methods. CsCl (99+%), Ta_2O_5 (98+%), TiO_2 (99.5+%), SeO_2 (99+%), and hydrofluoric acid (40+%, AR) were used as acquired. Chemicals were bought from the Shanghai Reagent Factory. The data of X-ray powder diffraction patterns were gathered on a Rigaku MiniFlex II diffractometer in the 2θ ambit of 5−65° with a step size of 0.02° at room temperature (Cu Kα radiation). The measurement of elemental analyses and the content of all elements were executed on a field emission scanning electron microscope (FESEM, JSM6700F) furnished with an energy dispersive X-ray spectroscope (EDS, Oxford INCA). The collections of infrared spectra for the two new titled compounds were performed on a Magna 750 FT-IR spectrometer with pure KBr pellets as a measure for the baseline correction over the scope 4000−400 cm^{-1} with a resolution of 2 cm^{-1} at 298 K. The UV−vis absorption and diffuse reflectance spectra were collected on PE Lambda 900 UV−vis−NIR spectrophotometer over 190−2500 nm at 298 K with analytically pure $BaSO_4$ as a standard for the baseline correction. Furthermore, the reflectance spectra were converted using the Kubelka−Munk function, $\alpha/S = (1 - R)^2/2R = K/S$,[12] where α, R, S, and K represent absorption coefficient, reflectance, scattering coefficient, and absorption, respectively, in order to ascertain the band gaps of the title compounds. The curves of thermogravimetric analysis (TGA) and differential scanning calorimetry (DSC) were measured on a NETZCH STA449C instrument with a heating rate of 10 °C/min under inert N_2 atmosphere. The SHG measurements for $Cs(TiOF)_3(SeO_3)_2$ were performed by a pulsed Nd:YAG laser on powder samples with a wavelength of 1064 nm at 298 K.[13] As the SHG response of the sample is known to strongly depend on its particle size, all powder samples of $Cs(TiOF)_3(SeO_3)_2$ were ground and sieved into a series of different particle sizes of 25−44, 44−53, 53−74, 74−105, 105−149, and 149−210 μm. KDP was used as reference to survey their SHG effect.

Preparation of $Cs(TaO_2)_3(SeO_3)_2$. $Cs(TaO_2)_3(SeO_3)_2$ was prepared by a standard high temperature solid-state method. A mixture, including CsCl (0.1348 g, 0.8 mmol), Ta_2O_5 (0.0884 g, 0.2 mmol), and SeO_2 (0.2219 g, 2.0 mmol), was ground thoroughly and then made into a pellet in order to guarantee the best reactivity and homogeneity. This pellet was introduced into a silica tube, which was sealed under vacuum environment. This silica tube was heated to 780 °C slowly and retained for 5 days. Then, the furnace was turned off after decreasing the temperature to 300 °C with a rate of 4 °C/h. When the furnace cooled down, the silica tube was transferred out and then opened. Colorless flake-like crystals of $Cs(TaO_2)_3(SeO_3)_2$ were successfully gained with a yield of about 17% based on metallic Ta. After a single crystal with few defects was used to determine the structure, the pure phase is necessary. The mixture of $CsCl/Ta_2O_5/SeO_2$ in molar ratio of 4:1:10 was heated at 700 °C for 5 days in an evacuated silica tube. After the excessive CsCl and SeO_2 were washed away with deionized water, a colorless crystalline single phase was obtained with the yield up to 92% based on metallic Ta. The single phase was established by powder-XRD measurement (Supporting Information Figure S1a). Results of EDS on several single crystals of $Cs(TaO_2)_3(SeO_3)_2$ indicate an average molar ratio of Cs/Ta/Se of 1:2.96:2.13, which is consistent with that determined by single-crystal X-ray structural research.

Preparation of $Cs(TiOF)_3(SeO_3)_2$. $Cs(TiOF)_3(SeO_3)_2$ was prepared by hydrothermal reactions. The mixture composed by CsCl (0.1348 g, 0.8 mmol), TiO_2 (0.032 g, 0.4 mmol), SeO_2 (0.2441 g, 2.2 mmol), three drops of HF acid (~40%), and deionized water (3 mL) was stirred thoroughly and then sealed into an autoclave (20 mL), which was transferred into hydrothermal stove and heated at 230 °C for 5 days. The crystals of $Cs(TiOF)_3(SeO_3)_2$ were synthesized according to the following equation:

$$CsCl + 3TiO_2 + 2SeO_2 + 3HF \rightarrow Cs(TiOF)_3(SeO_3)_2 + HCl + H_2O \quad (1)$$

After the powder impurity was removed by distilled water washing, a colorless block-shaped crystalline sample of $Cs(TiOF)_3(SeO_3)_2$ was obtained as pure with the yield up to 86% based on metallic Ti. The pure phase has been established by X-ray diffraction (XRD) research (Supporting Information Figure S1b). Results of EDS on several single crystals of $Cs(TiOF)_3(SeO_3)_2$ present an average molar ratio of Cs/Ti/Se/F of 1:3.03:2.17:3.31, which is consistent with that determined by single-crystal X-ray structural study.

Single-Crystal Structure Determination. Colorless brick-like crystals of $Cs(TaO_2)_3(SeO_3)_2$ (0.21 × 0.18 × 0.11 mm^3) and $Cs(TiOF)_3(SeO_3)_2$ (0.18 × 0.16 × 0.11 mm^3) were taken for structural determination. SuperNova CCD diffractometer with Mo Kα radiation (λ = 0.710 73 Å) was used for data collections at room temperature. The data sets were corrected by multiscan method for polarization factors, Lorentz and absorption.[14a] Then, the crystal structures were established through the direct methods and refined by full-matrix least-squares fitting on F^2 using *SHELXL*-97.[14b] *PLATON* was used for checking possible missing symmetry elements, but nothing was found.[14c] For $Cs(TiOF)_3(SeO_3)_2$, the Flack parameter was refined to be −0.02(3), indicating the absolute structure is correct. On the basis of results from the bond valence calculations, both the (0.0835, 0.5417, 0.2855) and (−0.1245, 0.1245, 0.2162) sites exhibit bond valences of −1.35 if considered as F atoms and −1.56 to −1.58 if considered as O atoms; hence, both sites should be considered as mixed sites composed of both O and F atoms. The (0.0835, 0.5417, 0.2855) site is refined as O(3) and F(1) with $^2/_3$ and $^1/_3$ occupancy, respectively, whereas the (−0.1245, 0.1245, 0.2162) site is composed of F(2) and O(4) with $^2/_3$ and $^1/_3$ occupancy, respectively. Crystal structural data and crucial bond lengths are given in Tables 1 and 2, respectively. In Supporting Information, other crystallographic data about the compounds are listed.

Computational Descriptions. We have carried out the theoretical computation (including electronic and optical properties) for the SHG-active compound of $Cs(TiOF)_3(SeO_3)_2$ within the CASTEP program.[15] The exchange-correlation function of GGA-PBE was employed for our DFT calculations.[16] A cutoff of 850 eV and a k-point separation of 1/0.04 Å in the Brillouin zone were adopted. The pseudopotential was set as norm-conserving.[17] Cs-$5s^25p^66s^1$, Ti-$3d^24s^2$, Se-$4s^24p^4$, O-$2s^22p^4$, and F-$2s^22p^5$ were treated as valence electrons.

The dielectric function $\varepsilon(\omega)$ was calculated by the formula of ref 18, which has been used in our previous studies. Through $n^2(\omega) = \varepsilon(\omega)$, the refractive indices of $Cs(TiOF)_3(SeO_3)_2$ were calculated. The SHG coefficients were obtained by the method of independent-particle approximation and the frequency-dependent expressions given elsewhere.[19,20] For the above optical properties, the empty bands number of >200 was calculated to ensure the accuracy of refractive indices and SHG coefficients. Besides, a scissor operator was added to correct the conduction band energies in optical calculations.

DOI: 10.1021/acs.inorgchem.5b00052
Inorg. Chem. 2015, 54, 3875−3882

Table 1. Summary of Crystal Data and Structural Refinements for the Title Two Compounds

	$Cs(TaO_2)_3(SeO_3)_2$	$Cs(TiOF)_3(SeO_3)_2$
fw	1025.68	635.53
cryst syst	trigonal	hexagonal
space group	$P\bar{3}m1$	$P6_3mc$
a (Å)	5.5153(4)	7.2420(3)
b (Å)	5.5153(4)	7.2420(3)
c (Å)	10.571(2)	11.8152(7)
α (deg)	90	90
β (deg)	90	90
γ (deg)	120	120
V (Å^3)	278.47(6)	536.65(4)
Z	1	2
D_c (g cm^{-3})	6.116	3.933
μ(Mo Kα) (mm^{-1})	39.210	12.383
GOF on F^2	1.165	1.068
Flack factor		−0.02(3)
R1, wR2 [$I > 2\sigma(I)$][a]	0.0423, 0.1053	0.0228, 0.0488
R1, wR2 (all data)	0.0473, 0.1142	0.0269, 0.0512

[a] $R1 = \sum||F_o| - |F_c||/\sum|F_o|$, $wR2 = \{\sum w[(F_o)^2 - (F_c)^2]^2/\sum w[(F_o)^2]^2\}^{1/2}$.

RESULTS AND DISCUSSION

Syntheses. Two new cesium d^0-TM selenites, namely, $Cs(TaO_2)_3(SeO_3)_2$ and $Cs(TiOF)_3(SeO_3)_2$, were successfully prepared using standard high temperature solid-state reaction or hydrothermal reaction. CsCl and SeO_2 were used as the Cs and Se sources, respectively. Attempts to use CsF as the Cs source for the synthesis of $Cs(TiOF)_3(SeO_3)_2$ were tried but were unsuccessful. Hence, during the preparation of $Cs(TiOF)_3(SeO_3)_2$, HF played an important role, acting as pH mediator and mineralizer as well as the F source.

Structure of $Cs(TaO_2)_3(SeO_3)_2$. $Cs(TaO_2)_3(SeO_3)_2$ crystallizes in space group $P\bar{3}m1$. The framework of $Cs(TaO_2)_3(SeO_3)_2$ can be described as the 2D $[(TaO_2)_3(SeO_3)_2]^-$ sandwich-like layers in the ab-plane, which are separated by Cs^+ cations (Figure 1). Its asymmetric unit includes one Cs^+, one Se^{4+}, as well as two Ta^{5+} ions. The Se^{4+} cation adopts a ψ-SeO_3 asymmetric coordination environment with the lone-pair electrons occupying the opposite site of the three oxygen atoms, which was attributed to the SOJT effect. The Se−O bond distances are 1.712(12) Å (Table 2). Both Ta^{5+} ions are octahedral coordination with six oxygen atoms.[8f] The $Ta(1)O_6$ octahedron is composed of three oxo atoms (O(2)) and three O(1) atoms shared with $Se(1)O_3$ groups. The Ta(1)−O bonds consist of three long (2.123(12) Å) and three short (1.864(10) Å) (Table 2) bonds; hence, distortion of the $Ta(1)O_6$ octahedron directs a face (local C_3 direction). To better understand, the degree of distortion (Δd) was calculated to be 0.784,[21] which approximates those for the NbO_6 and TaO_6 octahedra in $KNb_3Te_2O_{12}$ and $KTa_3Te_2O_{12}$.[8f] All six oxygen atoms of the $Ta(2)O_6$ octahedron came from six oxo anions (O(2)) with equal Ta−O bonds (1.959(10) Å) (Table 2); hence, no SOJT distortion occurred for $Ta(2)O_6$ octahedron.

The interconnection of $Ta(1)O_6$ octahedra and selenite groups resulted in the formation of a $[Ta(1)O_3(SeO_3)]^{3-}$ hexagonal layer in the ab-plane (Figure 1a). There are Ta_3Se_3 six member rings (MRs) in this layer. Two $[Ta(1)O_3(SeO_3)]^{3-}$ hexagonal layers are bridged by $Ta(2)O_6$ octahedra forming a 2D $[(TaO_2)_3(SeO_3)_2]^-$ sandwich-type double layer (Figure 1b). The $Ta(2)O_6$ octahedron is capping on two $Ta(1)_3Se_3$ 6-MRs. The above $[(TaO_2)_3(SeO_3)_2]^-$ sandwich-type double layers are separated by the counter Cs^+ cations (Figure 1c). The interlayer distance is 10.571(2) Å (about the length of the c-axis). The Cs^+ ion is 12-coordinated with 12 oxygen atoms, and all Cs−O bond lengths are equal to 3.319(7) Å (Table 2). Bond valence calculations for Cs^+, Ta^{5+}, and Se^{4+} ions resulted in values of 1.06, 5.22−5.40, and 3.92, proving the oxidation states of 1+, 5+, and 4+, respectively.[22]

Structure of $Cs(TiOF)_3(SeO_3)_2$. $Cs(TiOF)_3(SeO_3)_2$ crystallizes in polar space group $P6_3mc$. The average structure features HTO-type layers similar to that of $A(VO_2)_3(QO_3)_2$ (A = K, Tl, Rb, Cs, NH_4; Q = Se, Te). These HTO-type layers "capped" by QO_3 triangular pyramid from both sides are typical class **1** HTOs.[4a] In $Cs(TiOF)_3(SeO_3)_2$, TiO_4F_2 octahedra are interconnected via corner-sharing leading to an interesting 2D layer, which is "capped" by SeO_3 groups from both sides, forming a 2D $[(TiOF)_3(SeO_3)_2]^-$ anionic layer, and such neighboring layered structures are divided by Cs^+ ions (see Figure 2). Its asymmetrical unit of $Cs(TiOF)_3(SeO_3)_2$ contains one Cs, one Ti, two Se, two O/F mixed sites, and two O atoms. Among which, O(3) and F(1) atoms occupy the same position, namely O(3)F(1), whereas F(2) and O(4) atoms occupy another of the same positions, namely F(2)O(4). Hence, Ti^{4+} cation is in an asymmetrical octahedral coordination with two selenite oxygen atoms, two O(3)F(1) atoms, and two F(2)O(4) atoms due to the SOJT effect (Figure 2a). Each TiO_4F_2 octahedron is connected to four other TiO_4F_2 octahedra by O/F−Ti−O/F bonds. The range of Ti−O/F bond lengths is 1.923(3)−1.994(5) Å. The degree of the distortion (Δd) for TiO_4F_2 octahedron is calculated to be 0.082,[21] and it is much smaller than that for VO_6 octahedra in $Cs(VO_2)_3(SeO_3)_2$,[6c] TaO_6 in $Cs(TaO_2)_3(SeO_3)_2$, and TiO_5F in $Pb_2TiOF(SeO_3)_2Cl$.[11a] Both Se^{4+} cations are in ψ-SeO_3 asymmetric coordination geometry with the lone-pair electrons occupying the opposite site of the oxygen atoms. The scope of Se−O bond distances is in the 1.693(5)−1.710(5) Å range (Table 2).

Table 2. Selected Bond Distances (Å) for the Title Two Compounds

		$Cs(TaO_2)_3(SeO_3)_2$			
Cs(1)−O(1)	3.319(7) × 12	Ta(1)−O(1)	2.123(12) × 3	Se(1)−O(1)	1.712(12) × 3
Ta(1)−O(2)	1.864(10) × 3	Ta(2)−O(2)	1.959(10) × 6		
		$Cs(TiOF)_3(SeO_3)_2$			
Cs(1)−F(2)/O(4)	3.171(5) × 3	Ti(1)−O(3)/F(1)	1.923(3) × 2	Se(1)−O(1)	1.693(5) × 3
Cs(1)−O(1)	3.243(5) × 3	Ti(1)−F(2)/O(4)	1.932(2) × 2	Se(2)−O(2)	1.710(5) × 3
Cs(1)−O(3)/F(1)	3.655(6) × 3	Ti(1)−O(1)	1.933(5)		
Cs(1)−O(2)	3.675(9) × 3	Ti(1)−O(2)	1.994(5)		

DOI: 10.1021/acs.inorgchem.5b00052
Inorg. Chem. 2015, 54, 3875−3882

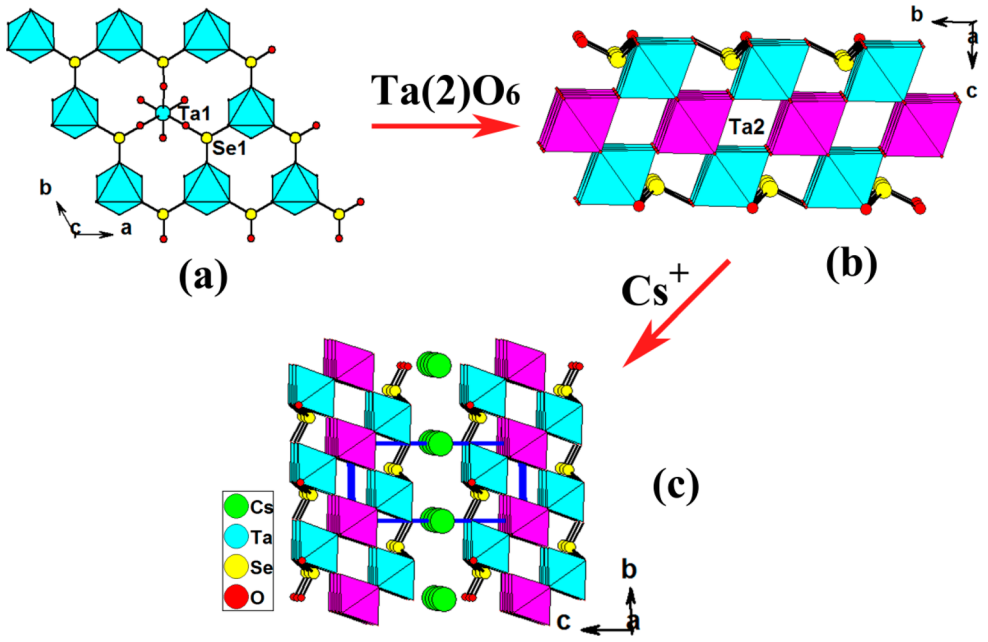

Figure 1. $Ta(1)O_3(SeO_3)$ layer in the *ab*-plane (a), a 2D $[(TaO_2)_3(SeO_3)_2]^-$ sandwich-type double layer in the *ab*-plane (b), and view of structure of $Cs(TaO_2)_3(SeO_3)_2$ down the *c*-axis. Cs, Se, and O atoms are drawn as green, yellow, and red circles, respectively. $Ta(1)O_6$ and $Ta(2)O_6$ octahedra are shaded in cyan and pink, respectively.

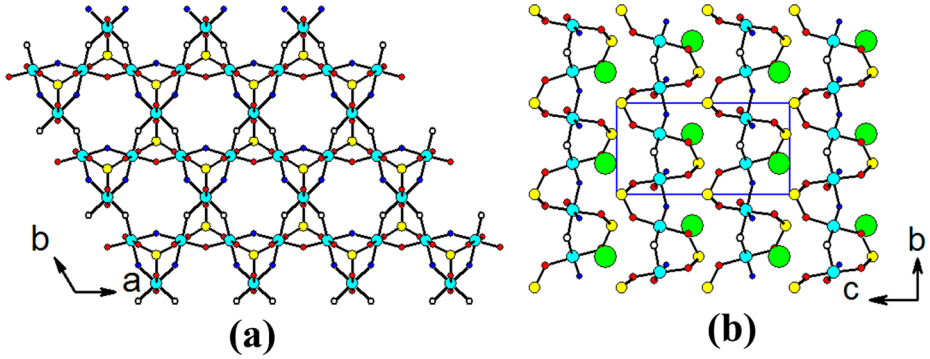

Figure 2. Two-dimensional $[(TiOF)_3(SeO_3)_2]^-$ anionic layer parallel to the *ab*-plane (a) and view of the structure of $Cs(TiOF)_3(SeO_3)_2$ down the *a*-axis (b). Cs, Ti, Se, O, O(3)F(1), and F(2)O(4) atoms are drawn as green, cyan, yellow, red, white, and blue circles, respectively.

The contiguous TiO_4F_2 octahedra are linked by corner-sharing (O(3)F(1) and F(2)O(4)) leading to a 2D anionic layered structure in *ab*-plane with 3- and 6-MRs. The 3-MRs are capped by SeO_3 groups, leading to the formation of a 2D $[(TiOF)_3(SeO_3)_2]^-$ anionic layer in the *ab*-plane (Figure 2a). The distance of these neighboring layers is 5.908(7) Å (about *c*/2). Such neighboring layers are separated by the counter Cs^+ cations (Figure 2b). The Cs^+ ion is 12-coordinated with nine oxygen and three fluorine atoms with Cs−O/F bond lengths in the scope 3.171(5)−3.675(9) Å. The valence for Cs^+, Ti^{4+}, and Se^{4+} ions has been calculated and gave the results of 0.84, 4.09, and 3.94−4.13, respectively, declaring the oxidation states of 1+, 5+, and 4+, respectively.[22]

The structures of $Cs(TiOF)_3(SeO_3)_2$ and $Cs(VO_2)_3(SeO_3)_2$ previously reported[6c] exhibit similar class **1** HTO-type layered topology; therefore, it is indispensable to compare their layered structure. The Ti−O/F bonds are five normal and one long; hence, the distortion of TiO_4F_2 octahedron directs a corner (local C_4 direction), and the degree of the distortion (Δd) is calculated to be very small (0.082). The V−O bonds in $Cs(VO_2)_3(SeO_3)_2$ are two long, two short, and two normal, and the degree of the distortion (Δd) for VO_6 octahedron is calculated to be 1.124,[21] which is much larger than that for the TiO_4F_2 in $Cs(TiOF)_3(SeO_3)_2$.

Furthermore, though $Cs(TaO_2)_3(SeO_3)_2$ exhibits a chemical composition similar to those of $Cs(VO_2)_3(SeO_3)_2$ and $Cs(TiOF)_3(SeO_3)_2$, they feature two different types of layered structures. The Ta^{5+} cations in $Cs(TaO_2)_3(SeO_3)_2$ are in two different coordination environments whereas the d^0-TM cations in those two HTO materials display only one type of coordination geometry. The corner-sharing TaO_6 octahedra in $Cs(TaO_2)_3(SeO_3)_2$ form a thick 2D sheet structure having 1D four member ring tunnels down the *a*-axis whereas TiO_4F_2 or VO_6 octahedra in the latter form a single layer with 3- and 6-MRs (Supporting Information Figure S2). In addition, the orientation of the lone-pair for Se^{4+} cation is different. Each SeO_3 group in $Cs(TaO_2)_3(SeO_3)_2$ bridges with three external Ta(1)O6 octahedra of the sandwich-type tantalum oxide layer; hence, its lone-pair is oriented inward of the sandwich-like layer (Figure 1b), whereas lone-pairs of the capping selenite groups in $Cs(VO_2)_3(SeO_3)_2$ and $Cs(TiOF)_3(SeO_3)_2$ are oriented outward of the HTO-type layer (Figure 2b).

DOI: 10.1021/acs.inorgchem.5b00052
Inorg. Chem. 2015, 54, 3875−3882

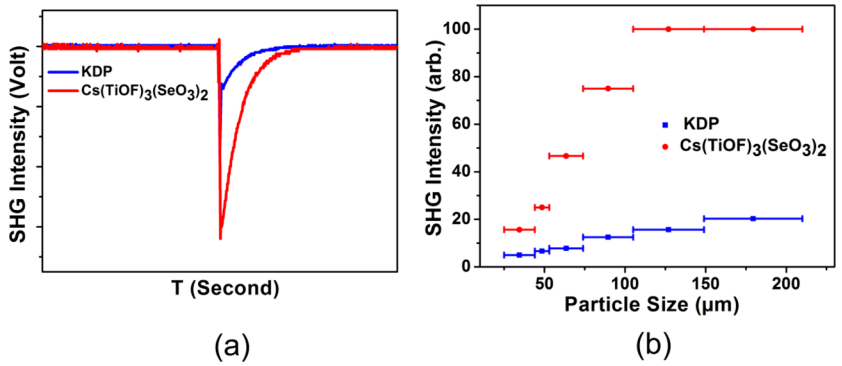

Figure 3. Oscilloscope traces of the SHG signals for the powders (149−210 μm) and phase-matching curve for KDP and $Cs(TiOF)_3(SeO_3)_2$ on a 1064 nm Q-switched Nd:YAG laser. The curve drawn is to guide the eye and not a fit to the data.

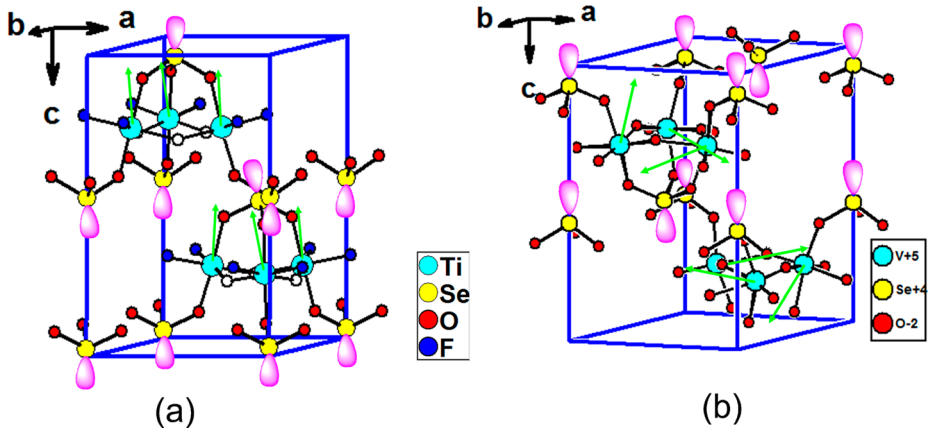

Figure 4. Ball-and-stick representations of (a) $Cs(TiOF)_3(SeO_3)_2$ and (b) $Cs(VO_2)_3(SeO_3)_2$. The green arrows indicate the approximate directions of the dipole moments of the TiO_4F_2 and VO_6 polyhedra in the unit cell. The cone-like isosurfaces near the top of SeO_3 polyhedra are consistent with a stereoactive lone-pair on the Se^{4+} cations. The Cs^+ cations have been removed for clarity.

Thermal Analysis. Curve analyses of TGA and DSC explain that $Cs(TaO_2)_3(SeO_3)_2$ and $Cs(TiOF)_3(SeO_3)_2$ can be stable below 708 and 420 °C, respectively (Supporting Information Figure S3). $Cs(TaO_2)_3(SeO_3)_2$ presents one main step of weight reduction during the scope of 708−1000 °C, exhibiting one endothermal peak around 832 °C in its DSC curve. The weight loss of 19.0% is consistent with the release of all selenium in the form of SeO_2 (calculated value: 21.6%).

TGA curve of $Cs(TiOF)_3(SeO_3)_2$ presents two steps of weight reduction at 310−893 °C and exhibits four endothermic peaks at 483, 536, 736, and 846 °C in its DSC curve. The weight loss of 35.0% for the first step is consistent with the release of the SeO_2 (calculated value: 34.9%). The weight loss for the second step is consistent with further decomposition of the compound.

Optical Measurements. The measurements of IR spectra of $Cs(TaO_2)_3(SeO_3)_2$ and $Cs(TiOF)_3(SeO_3)_2$ were performed in wavelength scope 4000−400 cm^{-1} at 298 K (Supporting Information Figure S4). $Cs(TaO_2)_3(SeO_3)_2$ and $Cs(TiOF)_3(SeO_3)_2$ show no absorption bands in the region 4000−1000 cm^{-1}, which also indicates there is no hydroxy in the structure of $Cs(TiOF)_3(SeO_3)_2$. In addition, they show a few absorption bands at 400−1000 cm^{-1} attributed to Ta−O, Ti−O(F), Se−O, and Se−O−Se (Supporting Information Table S1).[8f,11a] The absorption band around 990 cm^{-1} should belong to the Ta−O vibration, whereas the band at 894 cm^{-1} belongs to the Ti−O/F vibration; moreover, the bands around 652, 696, and 441 cm^{-1} belong to ν(Se−O−Se) and ν(Se−O).[8,11]

UV−vis absorption spectral studies of $Cs(TaO_2)_3(SeO_3)_2$ and $Cs(TiOF)_3(SeO_3)_2$ show no absorption at 366−2500 and 416−2500 nm, respectively (Supporting Information Figure S5). The results of the diffuse reflectance spectra reveal wide band gaps of about 3.88 and 3.50 eV for $Cs(TaO_2)_3(SeO_3)_2$ and $Cs(TiOF)_3(SeO_3)_2$ (Supporting Information Figure S6), respectively, indicating they are both wide band gap semiconductors.

SHG Measurements. The polar structure of $Cs(TiOF)_3(SeO_3)_2$ indicates the necessity to examine its SHG response. Comparison of SHG measurements on the $Cs(TiOF)_3(SeO_3)_2$ and KDP powders in the particle size 150−210 μm gave the result that $Cs(TiOF)_3(SeO_3)_2$ presents a large SHG of about 5 × KDP, and the measurements on different particle sizes of powders show it is type-I phase-matching (Figure 3). The large SHG response observed for $Cs(TiOF)_3(SeO_3)_2$ is mainly due to the polarizations from both TiO_4F_2 distorted octahedra and lone-pair containing selenite groups. The isostructural $Cs(VO_2)_3(SeO_3)_2$ previously reported only presents a slight SHG of about 40 × α-SiO_2. (It is closed to one time of KDP.)[4b]

To better understand the great difference of SHG effects for $Cs(TiOF)_3(SeO_3)_2$ and $Cs(VO_2)_3(SeO_3)_2$, the dipole moments for the unit cells of the two polar compounds have been calculated.[23,24] The dipole moments of asymmetric building units TiO_4F_2, VO_6, and SeO_3 polyhedra are 0.601, 9.460, and

DOI: 10.1021/acs.inorgchem.5b00052
Inorg. Chem. 2015, 54, 3875−3882

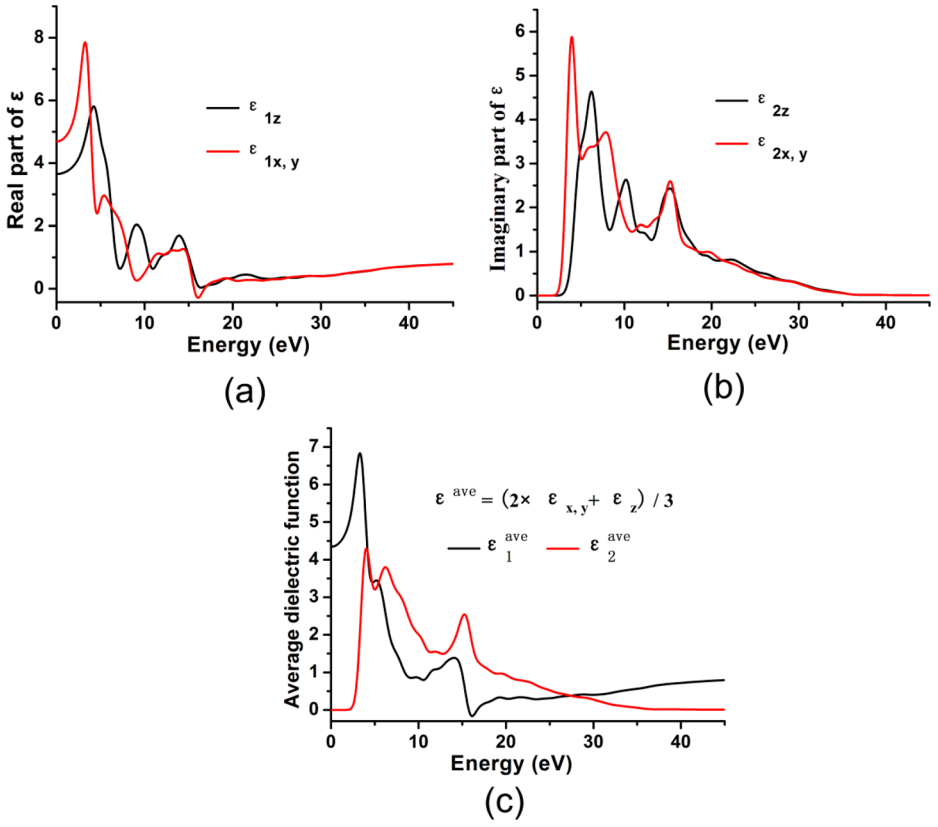

Figure 5. Imaginary and real parts of the dielectric function polarized along different directions (a, b), as well as the average dielectric function over different dielectric axes directions (c) for $Cs(TiOF)_3(SeO_3)_2$.

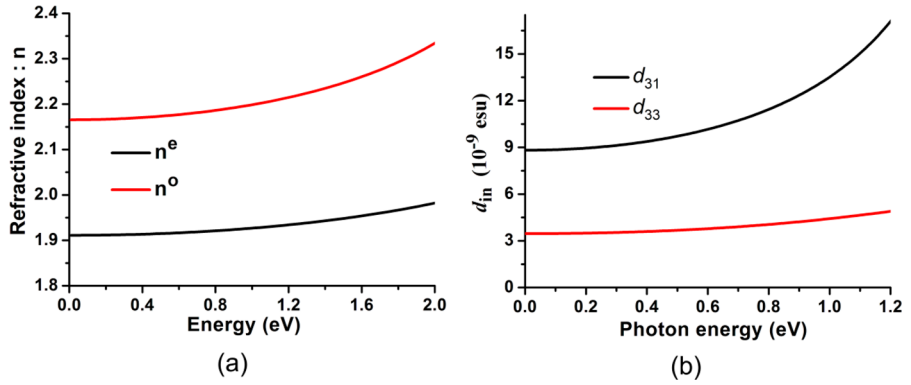

Figure 6. Calculated linear refractive indices (a) and frequency-dependent second harmonic generation coefficients (b) for $Cs(TiOF)_3(SeO_3)_2$.

7.491−8.873 D, respectively (Supporting Information Table S2), which are close to the previously reported values.[8] However, the net dipole moments along *x*- and *y*-axes from all asymmetrical building units canceled out completely. Down the polar *z*-axis, the dipole moments for all polar units are constructively added in unit cell for both compounds (Figure 4). For $Cs(TiOF)_3(SeO_3)_2$, the polarizations of *z*-components for TiO_4F_2, $Se(1)O_3$, and $Se(2)O_3$ polyhedra are 6 × (−0.340), 2 × (−8.873), and 2 × 7.954 D, respectively, constructively added to a value of −3.878 D for a unit cell. For $Cs(VO_2)_3(SeO_3)_2$, the polarizations of *z*-components for VO_6, $Se(1)O_3$, and $Se(2)O_3$ polyhedra are 6 × (−0.087), 2 × (−7.491), and 2 × 7.666 D, respectively, leading to a small value of −0.172 D for a unit cell. Hence, although both values are small, that net dipole moment of $Cs(TiOF)_3(SeO_3)_2$ is much larger than that of $Cs(VO_2)_3(SeO_3)_2$. Furthermore, the presence of F^- in the coordination geometry around the Ti^{4+} cation also provides a large SHG enhancement for the material according to our previous studies on other related systems.[11a] In addition, the much deeper color of $Cs(VO_2)_3(SeO_3)_2$ compared with that of $Cs(TiOF)_3(SeO_3)_2$ may also lead to much weaker SHG response under our measurement conditions.

Theoretical Results. *Band Structure.* Supporting Information Figure S7a displays the band structure of $Cs(TiOF)_3(SeO_3)_2$, and Supporting Information Table S3 lists the state energies of two special bands on each side of the gap. From Supporting Information Figure S7a and Table S3, we know that $Cs(TiOF)_3(SeO_3)_2$ has an indirect band gap of 3.10 eV, smaller than the measured one (3.50 eV). The underestimation is very common because of the limitation of the exchange-correlation function we used.[25] Therefore, a scissor of

DOI: 10.1021/acs.inorgchem.5b00052
Inorg. Chem. 2015, 54, 3875−3882

0.40 eV was adopted when analyzing the optical properties of $Cs(TiOF)_3(SeO_3)_2$.

Density of States. The density of states of $Cs(TiOF)_3(SeO_3)_2$ is displayed in Supporting Information Figure S7b, from which the bands can be assigned. Clearly, the valence bands of −23.6 to −9.8 eV are from F-2s, O-2s, Cs-5s, and Se-4s4p states. The valence bands near the gap are dominated by O-2p. In the regions −7.2 to 0 and 2.6−8.1 eV, there is full overlap among O-2p, Se-4p, F-2p, and Ti-3d states, implying strong interactions in Se−O, Ti−O, and Ti−F bonds for the compound. In addition, the peak at −6.2 eV arises from Cs-5p, and the dispersive bands of 8.1−20 eV can be attributed to Se-4s, Ti-4s4p, and Cs-6s6p states.

Linear Optical Properties. As shown in Figure 5a,b, the dispersive complex dielectric functions of $Cs(TiOF)_3(SeO_3)_2$ exhibit strong anisotropy. The averaged dielectric functions over different directions are calculated and shown in Figure 5c, from which the averaged static dielectric constant $\varepsilon(0)$ is determined to be 4.34. The DOS graph reveals that the strongest adsorption peak at ∼4.0 eV of $\varepsilon_2^{av}(\omega)$ results from the interband transitions from O-2p to Ti-3d and Se-4p. The refractive indices dispersion curves show $n^o > n^e$ during 0−2 eV, indicating $Cs(TiOF)_3(SeO_3)_2$ is a negative uniaxial crystal (Figure 6a). More importantly, the birefringence of the compound is large (0.279 at 1064 nm), making it easier to achieve phase-matching.

SHG Coefficients. The SHG coefficients of $Cs(TiOF)_3(SeO_3)_2$ are calculated, and the frequency-dependent tensors are displayed in Figure 6b. For $Cs(TiOF)_3(SeO_3)_2$, due to the limitations of point group and Kleinman symmetry, there are two independent SHG tensors, d_{31} and d_{33}, which are calculated to be 1.63×10^{-8} and 4.80×10^{-9} esu at 1064 nm (1.165 eV), respectively. The calculated SHG coefficients are larger than the measured one (5 × KDP), which may be because the calculations are based on single-crystal details, while the experimental measurements are on powder samples, and usually single crystals give higher SHG effects than powder.

CONCLUSIONS

In brief, two new cesium mixed metal selenites, namely, $Cs(TaO_2)_3(SeO_3)_2$ (**1**) and $Cs(TiOF)_3(SeO_3)_2$ (**2**), have been prepared successfully. Compound **1** features a sandwich-type $[(TaO_2)_3(SeO_3)_2]^-$ anionic layer whereas the polar compound **2** exhibits a layered hexagonal tungsten oxide (HTO) topology. Furthermore, $Cs(TiOF)_3(SeO_3)_2$ (**2**) presents a strong SHG response of approximately 5 × KDP (KH_2PO_4), which is much larger than $A(VO_2)_3(QO_3)_2$ (A = K, Tl, Rb, Cs, NH_4; Q = Se, Te) with a similar HTO layered structure. The much stronger SHG response for $Cs(TiOF)_3(SeO_3)_2$ (**2**) may be due to the involvement of F in the coordination with Ti^{4+} cation and the much lighter color for $Cs(TiOF)_3(SeO_3)_2$ (**2**) compared with that of $A(VO_2)_3(QO_3)_2$ (A = K, Tl, Rb, Cs, NH_4; Q = Se, Te). For our further work, we think it is significant to continue exploiting the alkali/alkaline earth metal−(d^0-TM)−Se^{4+}−oxyfluoride systems. More novel crystals and integrated data will help us to further understand the essence so that the involvement of F can lead to the large SHG enhancement.

ASSOCIATED CONTENT

Supporting Information

X-ray crystallographic files in CIF format, XRD powder patterns, IR spectrum, UV spectrum, TGA and DSC curves, band structures, and DOS figures. This material is available free of charge via the Internet at http://pubs.acs.org.

AUTHOR INFORMATION

Corresponding Author

*E-mail: mjg@fjirsm.ac.cn. Fax: (+86)591-63173121.

Notes

The authors declare no competing financial interest.

ACKNOWLEDGMENTS

This work was supported by the National Natural Science Foundation of China (Grants 21231006, 21403232, 21203197, and 91222108).

REFERENCES

(1) (a) Zhang, W.-L.; Cheng, W.-D.; Zhang, H.; Geng, L.; Lin, C.-S.; He, Z.-Z. *J. Am. Chem. Soc.* **2010**, *132*, 1508−1509. (b) Pan, S.; Smit, J. P.; Watkins, B.; Marvel, M. R.; Stern, C. L.; Poeppelmeier, K. R. *J. Am. Chem. Soc.* **2006**, *128*, 11631−11634. (c) Huang, Y.-Z.; Wu, L.-M.; Wu, X.-T.; Li, L.-H.; Chen, L.; Zhang, Y.-F. *J. Am. Chem. Soc.* **2010**, *132*, 12788−12789.

(2) (a) Kim, S.-H.; Yeon, J.; Halasyamani, P. S. *Chem. Mater.* **2009**, *21*, 5335−5342. (b) Ok, K. M.; Halasyamani, P. S. *Angew. Chem., Int. Ed.* **2004**, *43*, 5489−5491. (c) Phanon, D.; Gautier-Luneau, I. *Angew. Chem., Int. Ed.* **2007**, *46*, 8488−8491.

(3) (a) Halasyamani, P. S. *Chem. Mater.* **2004**, *16*, 3586−3592. (b) Johnston, M. G.; Harrison, W. T. A. *Eur. J. Inorg. Chem.* **2011**, 2967−2974. (c) Bang, S.-e.; Lee, D. W.; Ok, K. M. *Inorg. Chem.* **2014**, *53*, 4756−4762. (d) Kim, Y. H.; Lee, D. W.; Ok, K. M. *Inorg. Chem.* **2014**, *53*, 1250−1256. (e) Harrison, W. T. A.; Dussack, L. L.; Jacobson, A. J. *Inorg. Chem.* **1994**, *33*, 6043−6049. (f) Harrison, W. T. A.; Dussack, L. L.; Jacobson, A. J. *J. Solid State Chem.* **1996**, *125*, 234−242.

(4) (a) Chang, H. Y.; Kim, S. W.; Halasyamani, P. S. *Chem. Mater.* **2010**, *22*, 3241−3250. (b) Chang, H. Y.; Kim, S. H.; Ok, K. M.; Halasyamani, P. S. *Chem. Mater.* **2009**, *21*, 1654−1662. (c) Goodey, J.; Ok, K. M.; Broussard, J.; Hofmann, C.; Escobedo, F. V.; Halasyamani, P. S. *J. Solid State Chem.* **2003**, *175*, 3−12. (d) Ahn, H. S.; Lee, D. W.; Ok, K. M. *Inorg. Chem.* **2013**, *52*, 12726−12730. (e) Lee, D. W.; Ok, K. M. *Inorg. Chem.* **2013**, *52*, 6236−6238.

(5) (a) Bierlein, J. D.; Arweiler, C. B. *Appl. Phys. Lett.* **1986**, *49*, 917−919. (b) Davis, M. E.; Lobo, R. F. *Chem. Mater.* **1992**, *4*, 756−768. (c) Venuto, P. B. *Microporous Mater.* **1994**, *2*, 297−411.

(6) (a) Vaughey, J. T.; Harrison, W. T. A.; Dussack, L. L.; Jacobson, A. J. *Inorg. Chem.* **1994**, *33*, 4370−4375. (b) Harrison, W. T. A.; Dussack, L. L.; Jacobson, A. J. *Acta Crystallogr., Sect. C* **1995**, *C51*, 2473−2476. (c) Harrison, W. T. A. *Acta Crystallogr., Sect. C* **2000**, *C56*, E422−E422. (d) Harrison, W. T. A.; Buttery, J. H. N. *Z. Anorg. Allg. Chem.* **2000**, *626*, 867−870. (e) Dussack, L. L.; Harrison, W. T. A.; Jacobson, A. J. *Mater. Res. Bull.* **1996**, *31*, 249−255. (f) Gerand, B.; Nowogrocki, G.; Guenot, J.; Figlarz, M. *J. Solid State Chem.* **1979**, *29*, 429−434.

(7) (a) Harrison, W. T. A.; Dussack, L. L.; Jacobson, A. J. *Inorg. Chem.* **1994**, *33*, 6043−6049. (b) Harrison, W. T. A.; Dussack, L. L.; Vogt, T.; Jacobson, A. J. *J. Solid State Chem.* **1995**, *120*, 112−120. (c) Harrison, W. T.; Dussack, L. L.; Vaughey, J. T.; Vogt, T.; Jacobson, A. J. *J. Mater. Chem.* **1996**, *6*, 81.

(8) (a) Mao, J.-G.; Jiang, H.-L.; Kong, F. *Inorg. Chem.* **2008**, *47*, 8498−8510. (b) Zhang, S. Y.; Hu, C. L.; Sun, C. F.; Mao, J. G. *Inorg. Chem.* **2010**, *49*, 11627−11636. (c) Li, P.-X.; Hu, C.-L.; Xu, X.; Wang, R.-Y.; Sun, C.-F.; Mao, J.-G. *Inorg. Chem.* **2010**, *49*, 4599−4605. (d) Jiang, H.-L.; Huang, S.-P.; Fan, Y.; Mao, J.-G.; Cheng, W.-D. *Chem.−Eur. J.* **2008**, *14*, 1972−1981. (e) Kong, F.; Huang, S. P.; Sun, Z. M.; Mao, J. G.; Cheng, W. D. *J. Am. Chem. Soc.* **2006**, *128*, 7750−7751. (f) Gu, Q.-H.; Hu, C.-L.; Zhang, J.-H.; Mao, J.-G. *Dalton Trans.* **2011**, *40*, 2562.

DOI: 10.1021/acs.inorgchem.5b00052
Inorg. Chem. 2015, 54, 3875−3882

(9) (a) Yeon, J.; Kim, S.-H.; Sau Doan, N.; Lee, H.; Halasyamani, P. S. *Inorg. Chem.* **2012**, *51*, 609−619. (b) Oh, S.-J.; Lee, D. W.; Ok, K. M. *Inorg. Chem.* **2012**, *51*, 5393−5399. (c) Lee, E. P.; Song, S. Y.; Lee, D. W.; Ok, K. M. *Inorg. Chem.* **2013**, *52*, 4097−4103. (d) Oh, S.-J.; Lee, D. W.; Ok, K. M. *Dalton Trans.* **2012**, *41*, 2995−3000.
(10) (a) Becker, R.; Johnsson, M.; Kremer, R.; Lemmens, P. *Solid State Sci.* **2003**, *5*, 1411−1416. (b) Johnsson, M.; Törnroos, K. W.; Mila, F.; Millet, P. *Chem. Mater.* **2000**, *12*, 2853−2857. (c) Millet, P.; Bastide, B.; Pashchenko, V.; Gnatchenko, S.; Gapon, V.; Ksari, Y.; Stepanov, A. *J. Mater. Chem.* **2001**, *11*, 1152−1157. (d) Johnsson, M.; Tornroos, K. W.; Lemmens, P.; Millet, P. *Chem. Mater.* **2003**, *15*, 68−73. (e) Jiang, H.-L.; Mao, J.-G. *Inorg. Chem.* **2006**, *45*, 7593−7599.
(11) (a) Cao, X.-L.; Hu, C.-L.; Xu, X.; Kong, F.; Mao, J.-G. *Chem. Commun.* **2013**, *49*, 9965−9967. (b) Cao, X.-L.; Kong, F.; Hu, C.-L.; Xu, X.; Mao, J.-G. *Inorg. Chem.* **2014**, *53*, 8816−8824. (c) Li, H.; Wu, H.; Su, X.; Yu, H.; Pan, S.; Yang, Z.; Lu, Y.; Han, J.; Poeppelmeier, K. R. *J. Mater. Chem. C* **2014**, *2*, 1704−1710. (d) Wu, H.; Yu, H.; Yang, Z.; Hou, X.; Su, X.; Pan, S.; Poeppelmeier, K. R.; Rondinelli, J. M. *J. Am. Chem. Soc.* **2013**, *135*, 4215−4218.
(12) Wendlandt, W. M.; Hecht, H. G. *Reflectance Spectroscopy*; Interscience: New York, 1966.
(13) Kurtz, S. K.; Perry, T. T. *J. Appl. Phys.* **1968**, *39*, 3798−3813.
(14) (a) *CrystalClear Version 1.3.5*; Rigaku Corp.: Woodlands, TX, 1999. (b) Sheldrick, G. M. *SHELXTL, Crystallographic Software Package, SHELXTL, Version 5.1*; Bruker-AXS: Madison, WI, 1998. (c) Spek, A. L. *PLATON*; Utrecht University: Utrecht, The Netherlands, 2001.
(15) (a) Milman, V.; Winkler, B.; White, J. A.; Pickard, C. J.; Payne, M. C.; Akhmatskaya, E. V.; Nobes, R. H. *Int. J. Quantum Chem.* **2000**, *77*, 895−910. (b) Segall, M. D.; Lindan, P. J. D.; Probert, M. J.; Pickard, C. J.; Hasnip, P. J.; Clark, S. J.; Payne, M. C. *J. Phys.: Condens. Matter* **2002**, *14*, 2717−2744.
(16) Perdew, J. P.; Burke, K.; Ernzerhof, M. *Phys. Rev. Lett.* **1996**, *77*, 3865−3868.
(17) Lin, J. S.; Qteish, A.; Payne, M. C.; Heine, V. *Phys. Rev. B* **1993**, *47*, 4174−4180.
(18) Bassani, F.; Parravicini, G. P. *Electronic States and Optical Transitions In Solids*; Pergamon Press Ltd.: Oxford, U.K., 1975; p 149.
(19) (a) Ghahramani, E.; Moss, D. J.; Sipe, J. E. *Phys. Rev. B* **1991**, *43*, 8990−9002. (b) Ghahramani, E.; Moss, D. J.; Sipe, J. E. *Phys. Rev. Lett.* **1990**, *64*, 2815−2818.
(20) (a) Duan, C. G.; Li, J.; Gu, Z. Q.; Wang, D. S. *Phys. Rev. B* **1999**, *60*, 9435−9443. (b) Guo, G. Y.; Chu, K. C.; Wang, D. S.; Duan, C. G. *Phys. Rev. B* **2004**, *69*, 205416. (c) Guo, G. Y.; Lin, J. C. *Phys. Rev. B* **2005**, *72*, 075416. (d) Guo, G. Y.; Lin, J. C. *Phys. Rev. B* **2008**, *77*, 049901.
(21) (a) Kim, J.-H.; Baek, J.; Halasyamani, P. S. *Chem. Mater.* **2007**, *19*, 5637−5641. (b) Ra, H. S.; Ok, K. M.; Halasyamani, P. S. *J. Am. Chem. Soc.* **2003**, *125*, 7764−7765. (c) Chi, E. O.; Ok, K. M.; Porter, Y.; Halasyamani, P. S. *Chem. Mater.* **2006**, *18*, 2070−2074.
(22) (a) Brese, N. E.; Okeeffe, M. *Acta Crystallogr., Sect. B* **1991**, *47*, 192−197. (b) Brown, I. D.; Altermatt, D. *Acta Crystallogr., Sect. B* **1985**, *41*, 240−244.
(23) Sau Doan, N.; Halasyamani, P. S. *Inorg. Chem.* **2012**, *51*, 9529−9538.
(24) (a) Lee, D. W.; Oh, S.-J.; Halasyamani, P. S.; Ok, K. M. *Inorg. Chem.* **2011**, *50*, 4473−4480. (b) Izumi, H. K.; Kirsch, J. E.; Stern, C. L.; Poeppelmeier, K. R. *Inorg. Chem.* **2005**, *44*, 884−895.
(25) (a) Godby, R. W.; Schluter, M.; Sham, L. J. *Phys. Rev. B* **1987**, *36*, 6497. (b) Jiang, H.-L.; Kong, F.; Mao, J.-G. *J. Solid State Chem.* **2007**, *180*, 1764−1769. (c) Okoye, C. M. I. *J. Phys.: Condens. Matter.* **2003**, *15*, 5945−5958. (d) Terki, R.; Bertrand, G.; Aourag, H. *Microelectron. Eng.* **2005**, *81*, 514−523.

DOI: 10.1021/acs.inorgchem.5b00052
Inorg. Chem. 2015, 54, 3875−3882